Computers and Concrete, *Vol. 14, No. 5 (2014) 613-633*
DOI: http://dx.doi.org/10.12989/cac.2014.14.5.613

Confining effect of concrete in double-skinned composite tubular columns

Deok Hee Won[1a], Taek Hee Han[1b], Seungjun Kim[2c], Jung-Hwa Lee[3d] and Young-Jong Kang[*3e]

[1]*Coastal Engineering, Korea Institute of Ocean Science and Technology, Ansan, 426-744, Republic of Korea*
[2]*Marine Research Institute, Samsung Heavy Industries Co. Ltd, 217 Munjin-ro Daejeon, 137-857, Republic of Korea*
[3]*Department of Architectural, Civil and Environmental Engineering, Korea University, 145 Anamro Seoul, 156-701, Republic of Korea*

(*Received December 9, 2013, Revised August 11, 2014, Accepted August 20, 2014*)

Abstract. A double-skinned composite tubular (DSCT) column, which consists of concrete and inner and outer tubes, was finally developed to overcome the weaknesses of concrete filled tube columns by reducing the self-weight of the column and confining the concrete triaxially. Research pertaining to the stiffness and strength of the column and the confining effect in a DSCT column has been carried out. However, detailed studies on the confining stress, especially the internal confining stress in a DSCT column, have not been carried out. Internal and external confining stresses should be evaluated to determine the effective confining stress in a DSCT column. In this paper, the confining stresses of concrete before and after insertion of an inner tube were studied using finite element analysis. The relationship between the internal or external confining stresses and the theoretical confining stress was investigated by parametric studies. New modified formulae for the yield and buckling failure conditions based on the formulae suggested by former researchers were proposed. Through analytical studies, the modified formulae were verified to be effective for economic and reasonable design of the inner tubes in a DSCT column under the same confining stress.

Keywords: concrete; concrete structures; concrete-filled hollow steel sections; confined concrete; finite elements method; non-linear analysis

1. Introduction

Columns are the substructures of building and bridges, and their seismic performance must be maximized to prevent any sudden collapse induced by extreme load events. To accomplish this, ductility in the plastic hinge regions of the columns must be increased. In general, a reinforced concrete (RC) column confines concrete within steel and is designed to provide sufficient

*Corresponding author, Professor, E-mail: yjkang@korea.ac.kr
[a]Ph.D., E-mail: thekeyone@kiost.ac
[b]Ph.D., E-mail: taekheehan@kiost.ac
[c]Ph.D., E-mail: rocksmell@gmail.com
[d]Ph.D Student, Email : qevno@korea.ac.kr

http://www.techno-press.org/?journal=cac&subpage=8 ISSN: 1598-8198 (Print), 1598-818X (Online)

transverse reinforcement in the form of a spiral or circular (rectangular) arrangement. Moreover, these arrangements enhance the ductility of the column to prevent the buckling of longitudinal reinforcement bars or shear failure. In a concrete-filled tubular (CFT) column, transverse reinforcement is provided via concrete wrapped by a steel tube. Compared with RC columns, CFT columns exhibit better seismic performance owing to strength enhancement via confinement by the tube. However, it can be costly when used as large substructures because of the increase in self-weight. The tubes in CFT column were used new material as fiber reinforced plastics (FRP) and glass fiber reinforced plastics (GFRP) as well as steel to increase its performance. [Andres W.C. *et al*.(2013), Bahrami A. *et al*.(2013), Rasheed H. A. *et al*.(2013), Shraideh M.S. *et al*. (2013), Shrestha R *et al*.(2013), Tsai H. C.(2013), Zhu W.C. *et al*.(2012)]

However, the use of CFT columns as substructures for large structures has some disadvantages. To support heavy superstructures, the required diameter of the column increases, increasing the total weight. Because of increasing self-weight of the column, the seismic performance could consequently decrease.

To overcome these disadvantages, centrifugal hollow concrete-filled steel tube (H-CFST) columns were developed by Tong *et al*. (2005). Because of the reduction in self-weight, the use of these columns decreases the dependency on design seismic force. However, H-CFST columns are characterized by poor ductility and strength because the concrete in the column is only biaxially confined. Furthermore, these columns can suffer from brittle failure because their inner face is not confined. For ensuring that the inner face is confined, a double-skinned composite tubular (DSCT) column was developed in the late 1980s (Shakir-Khalil *et al*. 1987). In this column, two steel tubes are arranged coaxially. A DSCT column based on the shape presented by Han *et al*. (2010) is shown in Fig. 1. In this column, concrete is filled between two coaxial double-steel tubes. After the introduction of DSCT columns by Shakir-Khalil *et al*. (1987), many studies on the structural behavior of the columns have been carried out. Wei *et al*. (1997) demonstrated that the strength of the column is significantly greater than the sum of the strengths of each component: concrete, inner tubes, and outer tubes. Additionally, they presented an empirical formula for column strength. Zhao *et al*. (2002) studied the strength and ductility of a DSCT column with a square cross section. Tao *et al*. (2004) investigated the strength and ductility of a column with a circular cross section. Han *et al*. (2010) defined the failure modes of the column and proposed a nonlinear concrete column model that included the confining effects. Most researchers agree that the axial strength of a DSCT column is greater than the sum of the strength of each component.

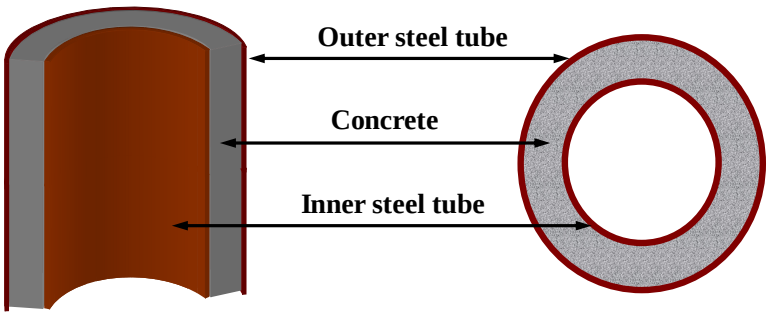

Fig. 1. Cross section of circular DSCT (Han *et al.* 2010)

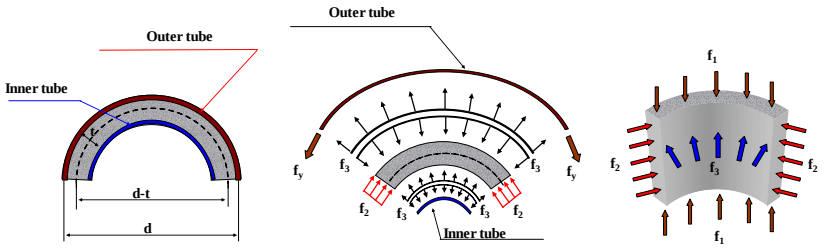

Fig. 2. Triaxially confined concrete in DSCT column (Han *et al*. 2010)

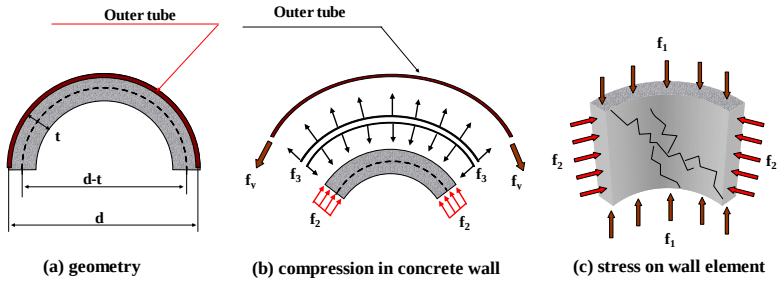

Fig. 3. Biaxially confined concrete (Han *et al*. 2010)

The main objective of this paper is to investigate the optimal confining effects on the concrete in DSCT columns. The confining mechanisms of concrete in DSCT and H-CFST columns are shown in Figs. 2 and 3, respectively (Han *et al*. 2010). Fig. 2 shows triaxially confined concrete in a DSCT column, and the parameters are defined as follows: d is the diameter of the confined concrete; t is the thickness of the concrete wall; f_1 is the axial pressure; f_2 is the circumferential pressure; f_3 is the radial pressure, which can be divided into the outer and inner radial pressures; and f_y is the yield stress of the outer tube. When concrete is subjected to a compressive force, it expands laterally according to the Poisson effect. Because concrete in a DSCT column is restrained by the inner and outer tubes, its volume cannot change freely, although it is subjected to an axial compressive force. In this situation, the tubes exert a lateral passive pressure (f_3) on the concrete in the radial direction. A circumferential pressure (f_2) is generated owing to the arching action of the concrete wall, as shown in Figs. 2(b) and 2(c). Fig. 3 shows an H-CFST column in which the concrete wall is biaxially confined because of the absence of an inner layer. When the concrete wall in an H-CFST column is subject to an axial pressure (f_1), a radial pressure is also directed inward via arching. Therefore, for estimating the optimal confining effect on concrete with respect to the confining condition, it is necessary to define reasonable inward and outward radial pressures in a DSCT column.

In this paper, the confining effects of concrete in DSCT and H-CFST columns were investigated and evaluated using ABAQUS, a commercial finite element analysis (FEA) tool. Parametric studies were performed to determine the factors affecting concrete confinement. Using the results of the parametric studies, new modified formulae for yield and buckling failure were proposed; these were based on the formulae suggested by Han *et al*. 2010.

2. Equilibrium and failure modes

Han *et al*. (2010) presented a basic theory on the force-equilibrium conditions and failure modes of a DSCT column. Their study was carried out under the following assumptions: 1) the inner tube provides complete confining pressure unless it fails; 2) the inner tube does not provide confining pressure if it fails; 3) the DSCT member fails when the outer tube fails; and 4) the concrete and tubes are not composite. The fourth assumption implies that the concrete is in an unconfined state when any tube fails.

2.1 Equilibrium in DSCT columns

Fig. 4 depicts the half section of a CFT column under axial loading that acts only on the concrete (Han *et al*. 2010). The confining pressure is maximized when the stress acting on the outer tube (f_{ot}) reaches the yield stress (f_{oty}). From Fig. 4, the constant confining pressure (f_l) can be calculated according to Eq. (1).

$$f_l = \frac{2 f_{oty} t_{ot}}{D'} \tag{1}$$

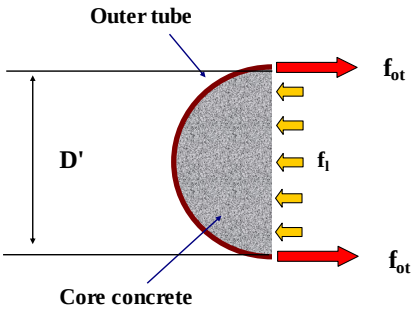

Fig. 4. Confining stress on concrete in CFT column (Han *et al*. 2010)

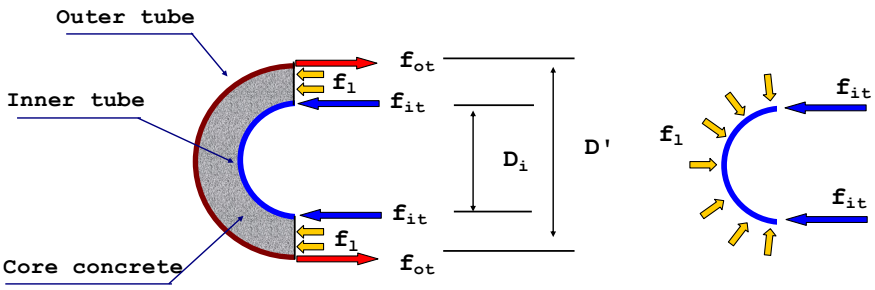

Fig. 5 Confining stress on concrete in DSCT column (Han *et al*. 2010)

where t_{ot} denotes the thickness of the outer tube, f_{oty} denotes the yield stress of the outer tube, and D' denotes the diameter of the confined concrete. The concrete in a CFT member is continuously confined along the height of the column by the outer tube.

In a DSCT column, the inner and outer tubes cooperatively provide continuous confining pressure to the concrete. Therefore, after one of the tubes fails, the concrete is in an unconfined state. Fig. 5 shows the free body diagram of the half section of a DSCT column under an axial load acting only on the concrete (Han *et al*. 2010). Eqs. (2) and (3) can be derived from Figs. 5(a) and 5(b), respectively. The stress acting on the inner tube (f_{it}) is calculated using Eq. (4), as derived from Eq. (3).

$$f_l(D'-D_i)+2f_{it}t_{it}=2f_{ot}t_{ot} \tag{2}$$

$$f_l D_i = 2t_{it} f_{it} \tag{3}$$

$$f_{it}=\frac{f_l D_i}{2t_{it}} \tag{4}$$

where t_{it} denotes the thickness of the inner tube and D_i denotes the outside diameter of the inner tube.

2.2 Failure modes

DSCT column failures are defined under three failure modes and can be expressed using Eq. (5), proposed by Han *et al*. 2010. The first failure mode is defined as the failure of the inner tube before the outer tube yields because of buckling or yielding. The reverse condition indicates the second failure mode. In the third failure mode, both tubes fail simultaneously.

$$f_{it} > f_{\lim} = smaller(f_{ity}, f_{bk}): \quad \text{Failure Mode 1} \tag{5a}$$

$$f_{it} < f_{\lim} = smaller(f_{ity}, f_{bk}): \quad \text{Failure Mode 2} \tag{5b}$$

$$f_{it} = f_{\lim} = smaller(f_{ity}, f_{bk}): \quad \text{Failure Mode 3} \tag{5c}$$

where f_{ity} is the yield strength of the inner tube, f_{bk} is the buckling strength of the inner tube, and $f_{\lim}$ is the smaller value between the yield and buckling strengths of the inner tube.

Optimal performance of a DSCT column is achieved when the inner tube does not fail before the outer tube yields. The yielding failure of the inner tube determines the limit of the concrete confining pressure induced by the tube. Additionally, the buckling of the inner tube leads to a loss of the confining pressure.

2.3 Yield conditions of inner tube

The prevention of the inner tube yielding prior to the outer tube can be controlled via the thickness of the inner tube. Eq. (6), which is derived from Eqs. (2) and (4), shows the relationship between the stresses acting on the inner and outer tubes. Therefore, Eq. (7) describes the prevention of the yielding failure of the inner tube before the failure of the outer tube. The

minimum required thickness of the inner tube to prevent premature yielding failure (t_y) is calculated using Eq. (8) (Han *et al*. 2010).

$$f_{it} = \frac{D_i t_{ot}}{D' t_{it}} f_{ot} \tag{6}$$

$$f_{it} = \frac{D_i t_{ot}}{D' t_{it}} f_{oty} < f_{ity} \tag{7}$$

$$t_y = \frac{D_i f_{oty}}{D' f_{ity}} t_{ot} \tag{8}$$

where f_{ity} denotes the yield stress of the inner tube and t_y denotes the required minimal thickness of the inner tube to prevent its premature yielding.

2.4 Buckling conditions of inner tube

The inner tube of a DSCT column is unilaterally restrained by concrete. This unilateral boundary condition changes the buckling strength of the inner tube; it is different from that of an arch or a ring with bilateral boundary conditions. The buckling strength of a unilaterally restrained arch was studied, resulting in the reporting of various buckling coefficients. The buckling behavior of the inner steel tube is considered as snap-through behavior of a circular shallow arch because the inner tube buckles inward only. For the inner tube, Han *et al*. (2010) adopted a buckling coefficient of 2.27, as proposed by Kerr *et al*. (1996). In their study, the buckling strength of a circular shallow arch (p_0) was calculated using Eq. (9). By substituting the snap-through buckling coefficient of 2.27 for the normalized non-dimensional pressure ($\overline{p}$) in Eq. (9), the buckling strength of the inner tube (f_{bk}) can be calculated according to Eq. (10).

$$p_0 = \overline{p} \frac{EI}{R^2 t_{ti}} \tag{9}$$

$$f_{bk} = 2.27 \frac{EI}{R^2 t_{it}} = \frac{2.27}{3} \frac{t_{it}^{\,2} E}{D_i^{\,2}} \tag{10}$$

where E is the modulus of elasticity, I is the moment of inertia, and R is the radius of the inner tube.

To prevent the premature buckling failure of the inner tube prior to that of the outer tube, the buckling strength of the inner tube must be larger than the confining pressure acting on the concrete when the outer tube yields. This design concept in combination with Eq. (10) provides the failure criterion as defined by Eq. (11). The required minimal thickness of the inner tube to prevent its premature buckling failure (t_{bk}) can be calculated by Eq. (12) (Han *et al*. 2010). Additionally, the required minimal thickness of the inner tube for the prevention of premature failure ($t_{\lim}$) is

Table 1 Failure criteria for DSCT columns (Han *et al*. 2010)

		Failure Mode	Stress criteria	Thickness criteria
1	A	Yielding of inner tube	$f_{it} > f_{\lim}$ and $f_{bk} > f_{ity}$	$t_{\lim} > t_{it}$ and $t_y > t_{bk}$
	B	Buckling of inner tube	$f_{it} > f_{\lim}$ and $f_{ity} > f_{bk}$	$t_{\lim} > t_{it}$ and $t_{bk} > t_y$
2		Yielding of outer tube	$f_{\lim} > f_{it}$	$t_{it} > t_{\lim}$
3		Simultaneous failure of two tubes	$f_{\lim} = f_{it}$	$t_{\lim} = t_{it}$

note; $f_{\lim} = \text{smaller}(f_{ity}, f_{bk})$, $t_{\lim} = \text{larger}(t_y, t_{bk})$

defined as the larger value between t_y and t_{bk} from Eqs. (8) and (12), respectively.

$$f_{bk} = \frac{2.27}{3}\frac{t_{it}{}^2 E}{D_i^2} > f_l = \frac{2 f_{oty} t_{ot}}{D'} \tag{11}$$

$$t_{bk} = \sqrt{\frac{6}{2.27}\frac{D_i^2 f_{oty} t_{ot}}{D' E}} \tag{12}$$

When a DSCT column fails via Failure mode 1, it can be ascribed to either yielding or buckling of the inner tube. The failure mode can be determined by comparing the yield strength (f_{ity}) of the inner tube to its buckling strength (f_{bk}). Additionally, it is possible to determine the failure mode by evaluating the thickness of the inner tube (t_{it}) and its required minimal thicknesses for yielding (t_y) and buckling (t_{bk}). Table 1 summarizes the failure criteria for a DSCT column (Han *et al*. 2010).

3. Finite element analysis

The confining effect in a DSCT column was investigated using FEA, and the results were validated against the testing data of CFT columns (Im *et al*. 2006). Numerical investigations were executed using ABAQUS.

3.1 Verification of finite element model

For a reasonable analytical study, numerical models should be validated using reliable analytical or experimental results. In this study, FEA of a DSCT column was employed; it was indirectly validated using test data of CFT columns under compressive loads. The modeling techniques for the concrete and steel are as follows. The concrete damaged plasticity model in ABAQUS was selected to represent the inelastic behavior of the concrete elements based on the assumption of isotropic damage. In this model, the degradation of elastic stiffness induced by tensile and compressive plastic straining is considered. Furthermore, the method provides a continuum and plasticity-based damage model for concrete. The two main failure mechanisms of

concrete are assumed to be tensile cracking and compressive crushing. The material parameters of the damaged concrete plasticity model are presented in Table 2, and the material parameters of the steel plastic model are presented in Table 3. For modeling steel tubes and filled concrete, shell element (S8R) and solid element (C3D8R) were used to model steel tubes and concrete, respectively. The contact mechanism between the steel tubes and concrete was assumed to be frictionless because the adhesion strength of the contact surface is negligible.

To verify the analysis models, two models were selected, as shown in Table 4. The first CFT column model consists of concrete with an unconfined strength of 30 MPa and a 1-mm-thick outer steel tube. The other CFT column consists of concrete with an unconfined strength of 23.9 MPa and a 0.8-mm-thick outer steel tube. Figs. 6 and 7 portray the applied material properties of concrete and steel, respectively. The loading and boundary conditions of the models are similar to

Table 2 Applied material and section properties of concrete

Concrete		Parameters of CDP model	
E, modulus of elasticity	25742	ψ, dilation angle	30°
ν, Poisson's ratio	0.18	ε, flow potential eccentricity	0.1
Density (kg/m3)	2403	$\sigma_{b0} / \sigma_{c0}$ *	1.16
Compressive strength MPa	23.9, 30	K_c **	0.667
Tensile strength MPa (psi)	2.8 (400)	μ, Viscosity parameter	0.0
Concrete compression hardening		Concrete tension stiffening	
Yield stress, MPa	Crushing strain	Remaining stress after cracking, MPa	Cracking strain
24	0.0	2	0.0
28 ~ 34	0.002	0	0.002
17	0.003	-	-

* Ratio of initial equibiaxial compressive yield stress to initial uniaxial compressive yield stress.
** Ratio of second stress invariant on tensile meridian, q (TM), to that on compressive meridian, q (CM).

Table 3 Applied material properties of steel

	E (GPa)	ν	Density (kg/m3)	Yield strength (MPa)
Steel tube	210	0.3	7850	250

Table 4 Dimensions of verification model

	Steel tube (mm)	Concrete (mm)
Diameter	102	100
Height	200	200
Thickness of tube	1 (0.8)	-

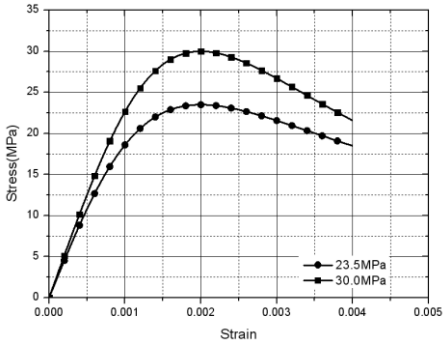

Fig. 6 Applied material model for concrete

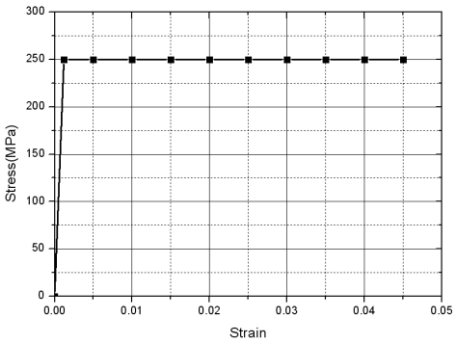

Fig. 7 Applied material model for steel tube

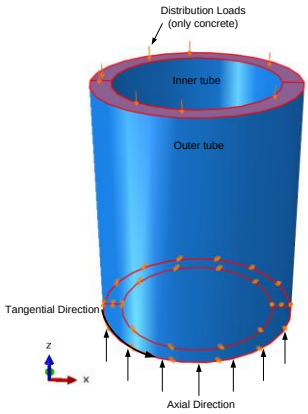

Fig. 8 Loading and boundary conditions of model

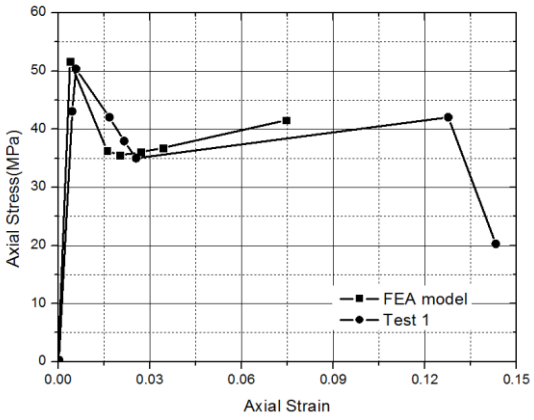

Fig. 9 Comparison of axial stresses obtained using FEA model and Test 1 (30 MPa, 1 mm)

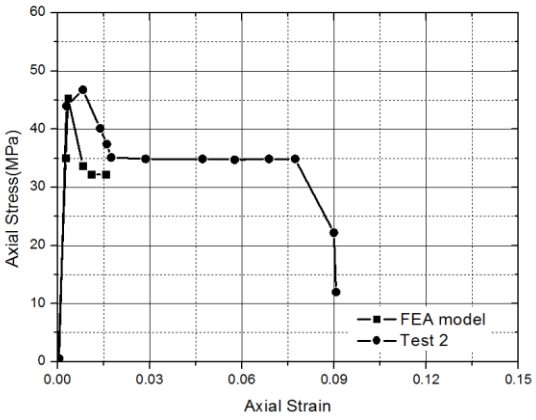

Fig. 10 Comparison of axial stresses obtained using FEA model and Test 2 (23.9 MPa, 0.8 mm)

those shown in Fig. 8. The bottom side of the model is fixed in the tangential and axial directions. The compressive load is applied only to the top of the concrete. The stress-strain curves from the FEA results were compared to the results of Im *et al*. (2006). As shown in Figs. 9 and 10, the FEA results agreed well with the test data results of Im *et al*. (2006), although the initial stiffness as determined by FEA is slightly higher than the stiffness from the test data. This gap in the initial stiffness values originates from insufficient information on material properties used in the test but not the FEA.

4. Confining stresses in DSCT columns

4.1 Confining stresses in H-CFST and DSCT columns

Determining the effective confining stress illuminates the compressive behavior of hollow columns. It is important to define the confining stress in hollow section columns, such as DSCT and H-CFST columns. The confining stress consists of an external confining stress (f_{ol}) and an internal confining stress (f_{il}). Han *et al*. (2010) assumed that these two types of stresses are equal at every point in the section of a column, as shown in Fig. 5. In reality, however, they have different values, although they are located in the same plane because of the arching action induced by its geometric characteristics. When the concrete of a DSCT column is subjected to a compressive force, the outer part of the concrete is confined by the outer tube while the inner part of the concrete is confined by the inner tube and the surrounding concrete. The confining stress applied by the inner tube is smaller than that applied by the outer tube because of the resistance pressure of the concrete in the inner direction.

To validate the above-mentioned mechanism, FEA was performed for the H-CFST and DSCT columns, in which they are subjected to compressive forces. Table 5 and 6 list the geometric and material properties of the analysis models. In the H-CFST column models, the hollow ratio (Di (inside diameter of confined concrete) / D'(outside diameter of confined concrete)) varies from 0.1

Table 5 Geometric and material properties of H-CFST columns

outside diameter (mm)	hollow ratio	inside diameter (mm)	thickness of outer tube (mm)	theoretical confining stress (MPa)
400	0.1	40	8	10.00
	0.2	80	8	10.00
	0.3	120	8	10.00
	0.4	160	8	10.00
	0.5	200	8	10.00
	0.6	240	8	10.00
	0.7	280	8	10.00
	0.8	320	8	10.00
	0.9	360	8	10.00

Table 6 Geometric and material properties of DSCT columns

outside diameter (mm)	hollow ratio	inside diameter (mm)	thickness of outer tube (mm)	thickness of inner tube (mm)	theoretical confining stress (MPa)
400	0.1	40	8	0.8	10.00
	0.2	80	8	1.6	10.00
	0.3	120	8	2.4	10.00
	0.4	160	8	3.2	10.00
	0.5	200	8	4	10.00
	0.6	240	8	4.8	10.00
	0.7	280	8	5.6	10.00
	0.8	320	8	6.4	10.00
	0.9	360	8	7.2	10.00

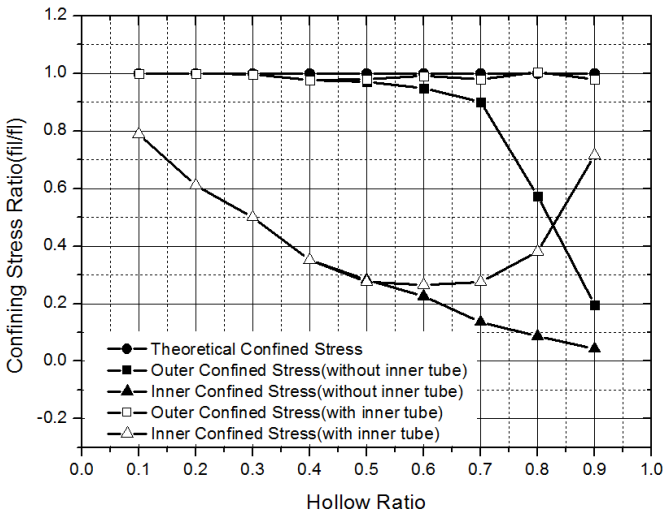

Fig. 11 Confining stress ratio with respect to hollow ratio for H-CFST and DSCT columns

to 0.9 and the theoretical confining stress was calculated by Eq. (1) for each hollow ratio. The geometric material properties of the DSCT column models are same as those of the H-CFST models, except for the thicknesses of the inner tubes. The inner tube thicknesses in each model were chosen to be the larger value between the two values calculated by Eqs. (8) and (12). Fig. 11 depicts the confining stress ratios (f_{il} / f_l) with respect to the hollow ratios of the H-CFST and DSCT columns. The external confining stress (f_{ol}) is approximately equal to the theoretical confining stress (f_l) until the hollow ratio reaches 0.3. As the hollow ratio increases beyond 0.3, the external confining stress (f_{ol}) of the H-CFST column slowly decreases until the hollow ratio reaches 0.7. The stress significantly decreases after the hollow ratio reaches 0.7. When the hollow

ratio is 0.9, the stress of the H-CFST columns is within 20% of the theoretical confining stress (f_l). In this case, the concrete is either in a biaxial confined state or an unconfined state because the effect of the arching action decreases with the change in geometric conditions. The internal confining stress (f_{il}) linearly decreases as the hollow ratio increases. For the DSCT column, the external confining stress (f_{ol}) is similar to the theoretical confining stress (f_l) for the entire range of hollow ratios. Also, the internal confining stress proportionally increases with the external confining stress because of the tube inserted inside the column. Likewise, when the inner tube is not inserted, the theoretical confining stress is different from the external or internal confining stress, as Eq. (13) dictates. However, when the inner tube is present, as for the DSCT column, the concrete in the column is triaxially confined. The theoretical confining stress is similar to the external confining stress but not the internal confining stress, as determined by Eq. (14). Therefore, an enhanced definition of the internal confining stress is required for the evaluation of the confining stress in a DSCT column.

$$f_l \neq f_{ol} \neq f_{il} \tag{13}$$

$$f_l \approx f_{ol} \neq f_{il} \tag{14}$$

The concrete confining in a DSCT column can be estimated by assuming the concrete is under a triaxially confined state because of the inner tube. An H-CFST column requires an inner tube in order to provide sufficient ductility and strength.

4.2 Parametric study

As shown in Fig. 1, a DSCT column consists of an outer tube, an inner tube, and concrete. The hollow ratio, the outer diameter of the column, the thickness of the inner tube, the bending stiffness of the outer tube, and the concrete were considered the main parameters that effect in the confining affect the column. The FEA models shown in Table 7 investigate the effects of the hollow ratio and the outer diameter of the column on the internal confining stress (f_{il}). The theoretical confining stress (f_l) was calculated using Eq. (1). The thickness of the inner tube was selected so that the inner and outer tubes yielded simultaneously via trial and error. Fig. 12 presents the change of the internal confining stress with respect to the outer diameter and the hollow ratio of a DSCT column. It demonstrates that the internal confining stress is significantly affected by the hollow ratio. Conversely, the variations of the outer diameter of the column and the theoretical confining stress have little affect the internal confining stress as compared to the strong effect of the hollow ratio.

Table 8 summarizes the dimensions of the FEA models with various bending stiffness ratios of the outer tubes and the concrete. The bending stiffness ratios were selected to be 1.19, 1.41, and 1.63, as in shown Table 8. In each major group of bending stiffness ratios in the table, subgroups are classified by the outer diameters of the columns. For all groups, hollow ratios within the range of 0.1 to 0.9 were considered, and the thickness of the inner tube was calculated by Eqs. (8) and (12).

As shown in Table 8, the theoretical confining stresses (f_l) for all analysis models were different. Fig. 13 shows the change of the internal confining stress with respect to the bending stiffness. In the hollow ratio range of 0.1 to 0.4, the confining stress ratio did not change significantly with respect to the bending stiffness ratio. When the hollow ratio surpasses 0.5, a significant difference exists between the confining stress ratios. The confining stress ratios with a

Table 7 Dimensions of analysis model for evaluating effects of diameter and hollow ratio on confining stress

Diameters (mm)	hollow ratio	thickness of outer tube (mm)	theoretical confining stress (MPa)
D300	0.1~0.9	4	6.67
D800	0.1~0.9	10	6.25
D1500	0.1~0.9	19	6.33
D2100	0.1~0.9	26	6.19
D2800	0.1~0.9	35	6.25

Table 8 Dimensions of FEA models for evaluating effects of bending stiffness between concrete and outer tube on confining stress

Bending stiffness	Diameters (mm)	hollow ratio	thickness of outer tube (mm)	theoretical confining stress (MPa)
1.19	D1500	0.1~0.9	19.0	6.33
	D2800	0.1~0.9	35.0	6.25
1.41	D1500	0.1~0.9	22.0	7.33
	D2800	0.1~0.9	41.0	7.32
1.63	D1500	0.1~0.9	25.1	8.37
	D2800	0.1~0.9	47.0	8.39

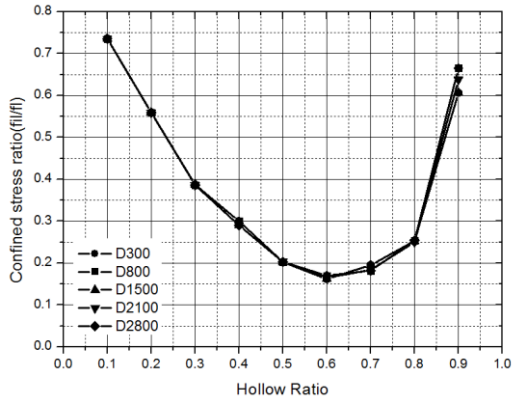

Fig. 12. Relationship of hollow ratio to confining stress ratio for various outer diameters of columns

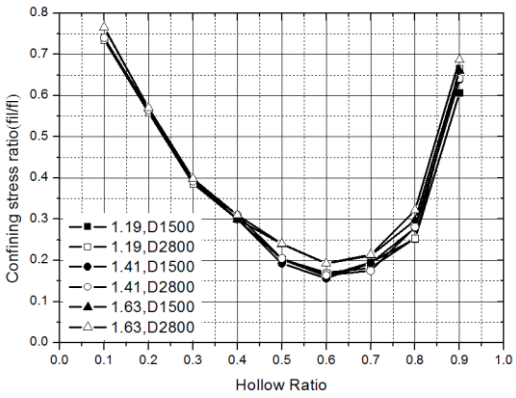

Fig. 13. Relationship of hollow ratio to confining stress ratio for various bending stiffness values and outer diameters of columns

bending stiffness of 1.19 and 1.41 had similar values although the diameters of the columns were different. However, the confining stress ratio with the bending stiffness ratio of 1.63 was a somewhat larger than another that of the 1.41 bending stiffness ratio.

Table 9 shows the dimensions of the FEA models, which were designed to include different thicknesses of inner tubes. All parameters are the same as the aforementioned models, excluding the thickness of the inner tubes, which varied between 13 mm and 40 mm. Fig. 14 depicts the

Table 9 Dimensions of FEA models for evaluating effect of inner tube thickness on confining stress

Diameters (mm)	hollow ratio	thickness of outer tube (mm)	thickness of inner tube (mm)
D2800	0.8	35	16~40

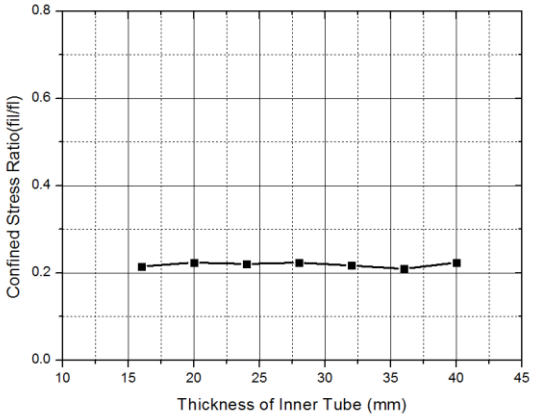

Fig. 14. Internal confining stress with respect to inner tube thickness

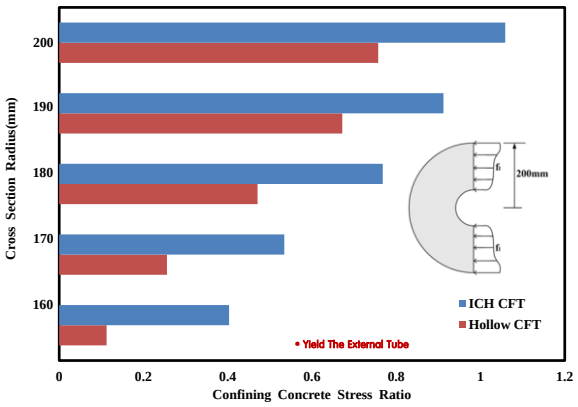

Fig. 15. Distributions of concrete confining stresses in DSCT and H-CFST columns

change of the internal confining stress with respect to the inner tube thickness. The internal confining stresses of all analysis models were within approximately 23% of the theoretical confining stresses. When the inner tube has a sufficient recommended thickness, the internal confining stress is negligibly affected by the change of inner tube thickness. Additionally, the distribution of the confining stresses in a DSCT column was investigated, as shown in Fig. 15. In the diagram, the analysis results of the model in Table 6 with a hollow ratio of 0.8 were used. As shown in the figure, the distribution of the confining stress exhibits a nonlinear distribution pattern because of the material and geometric nonlinearities. Therefore, the distribution of the confining stress of hollow section columns should be considered to be nonlinear.

As shown in these parametric studies, the hollow ratio has the strongest effect on the internal confining stress than any other factors that were considered in this study. Therefore, modified equations for the yield and buckling conditions of an inner tube that consider the effective internal confining stress are required.

5. Modified failure conditions

Through the analytical results, the ratio of the internal confining stress (f_{il}) to the theoretical confining stress (f_l) was determined. Furthermore, the failure conditions suggested by Han *et al*. (2010) were modified using the relationship between the two stresses. Also, a modified confining stress on the concrete was proposed for the DSCT columns.

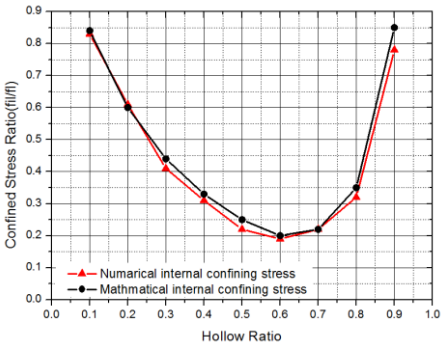

Fig. 16. Numerical versus mathematical internal confining stresses with respect to hollow ratio

5.1 Internal confining stress from mathematical and numerical results

According to the parametric studies, the hollow ratio is the main factor that affects the internal confining stress (f_{il}) in a DSCT column. The relationship between the theoretical external confining stress (f_l) and the internal confining stress (f_{il}) can be represented by a reduction coefficient (γ), as shown in Eq. (15). The reduction coefficient (γ) is expressed in two separate equations based on the hollow ratio, as defined by Eqs. (16) and (17), which define the internal confining stress in a DSCT column. The mathematical internal confining stresses as determined by Eqs. (15)-(17) have similar tendencies as the numerical internal confining stresses as determined by FEA, as demonstrated in Fig. 16.

$$f_{il} = \gamma f_l \tag{15}$$

$$\gamma_{0.1\le x\le 0.6} = 0.09 + 1.1e^{-x/0.26} \tag{16}$$

$$\gamma_{0.6<x\le 0.9} = 0.18 + (2.5\times 10^{-6})e^{x/0.072} \tag{17}$$

where x is the hollow ratio, (D_i / D').

5.2 Modified yield failure conditions of inner tube

For a feasible design, the external and internal confining stresses should be defined separately, as shown in Fig. 17, which demonstrates the modified confining stresses on the concrete in a DSCT column. First, the external confining stress (f_{ol}) can be expressed as shown in Eq. (18) because it is assumed to be the same as the theoretical confining stress (f_l).

$$f_l = f_{ol} = \frac{2 f_{oty} t_{ot}}{D'} \tag{18}$$

where t_{ot} denotes the thickness of the outer tube, f_{oty} is the yield stress of the outer tube, and D' is the diameter of confined concrete.

The internal confining stress (f_{il}) is calculated by Eq. (19). Also, it can be expressed with the theoretical confining stress (f_l), as shown in Eq. (20).

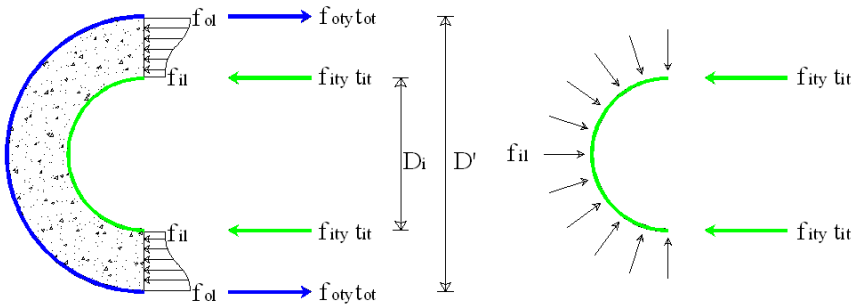

Fig. 17. Modified concrete confining stress in DSCT columns

$$f_{il} = \frac{2t_{it}}{D_i} f_{ity} \tag{19}$$

$$f_{il} = \gamma f_l = \frac{2t_{it}}{D_i} f_{ity} \tag{20}$$

where f_{ity} is the yield stress of the inner tube, t_{it} is the thickness of the inner tube, and D_i is the outside diameter of the inner tube.

The theoretical confining stress (f_l) is expressed as

$$f_l = \frac{2 f_{ity} t_{it}}{\gamma D_i} \tag{21}$$

Therefore, from Eq. (1), the theoretical confining stress on the concrete is written as

$$f_l = \frac{2 f_{oty} t_{ot}}{D'} = \frac{2t_{it} f_{ity}}{\gamma D_i} \tag{22}$$

From Eq. (22), the minimal required thickness (t_y) of the inner tube to prevent its premature yielding failure is derived as

$$t_{it} = \frac{\gamma t_{ot} f_{oty} D_i}{f_{ity} D'}, \quad t_y > \frac{\gamma t_{ot} f_{oty} D_i}{f_{ity} D'} \tag{23}$$

where t_y denotes the required minimal thickness of the inner tube to prevent its premature yielding.

5.3 Modified buckling failure conditions of inner tube

To prevent premature buckling failure of the inner tube, the buckling strength of the inner tube should be larger than the internal confining stress acting on inner tube.

$$f_{bk} > f_{il} \tag{24}$$

Substituting Eq. (10) and Eq. (15) into f_{bk} and f_l in Eq. (24), respectively, the following

equation can be obtained.

$$\frac{2.27}{3}\frac{t_{it}^2 E}{D_i^2} > \gamma f_l \tag{25}$$

Substituting Eq. (1) into f_l in Eq. (25), the equation is written as

$$\frac{2.27}{3}\frac{t_{it}^2 E}{D_i^2} > \frac{\gamma 2 f_{oty} t_{ot}}{D'} \tag{26}$$

Rearranging Eq. (26), the required minimal thickness of the inner tube to prevent its bucking failure can be calculated as

$$t_{bk} > \sqrt{\frac{6}{2.27}\frac{\gamma D_i^2 f_{oty} t_{ot}}{D' E}} \tag{27}$$

5.4 Verification of modified equations

The modified equations were verified using FEA models under various conditions. The thickness of the inner tube was calculated by the modified equations so that the failure of the inner tube does not occur before failure of the outer tube. Table 10 shows the dimensions of the FEA models for verification. As shown in the table, the verification models are classified into six groups by the outer diameter. Also, a range of hollow ratio ranges from 0.1 to 0.9 was considered for each group. The thickness of the inner tubes was selected as the larger value between the thicknesses calculated from Eq. (23) and (27). The material properties from Tables 2 and 3 were applied to the models.

Fig. 18 presents the ratio between the numerical internal confining stress as determined by FEA and the mathematical internal confining stress as determined by Eqs. (15)–(17). The numerical internal confining stresses are distributed in the range of 70–90% against the mathematical internal confining stresses. The mathematical internal confining stresses are more conservative than the numerical internal confining stresses and therefore provide a safer design.

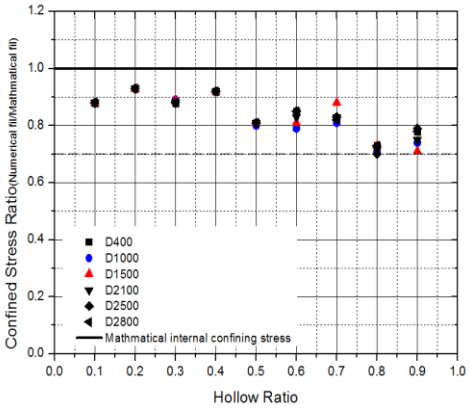

Fig. 18. Comparison of numerical and mathematical internal confining stresses with respect to hollow ratio for various dimensions

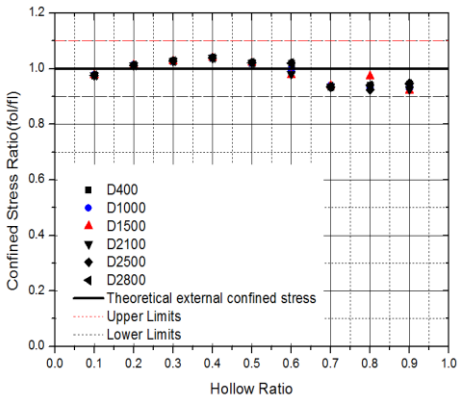

Fig. 19. Comparison of numerical and theoretical external confining stresses with respect to hollow ratio for various dimensions

Table 10 Dimensions of FEA models for verifying modified equations

Diameters (mm)	hollow ratio	thickness of external tube (mm)	thickness of internal tube (mm)
D400	0.1~0.9	5	0.5~3.9
D1000	0.1~0.9	13	1.2~10.1
D1500	0.1~0.9	19	1.7~14.8
D2100	0.1~0.9	26	2.3~20.2
D2500	0.1~0.9	31	2.7~24.1
D2800	0.1~0.9	35	3.1~27.2

Table 11 Yield stresses on inner tube when outer tube yields (hollow ratio of 0.8)

Diameters	yield stress of outer tube (MPa)	stress acting on inner tube (MPa)
D400	250	36.4
D1000	250	52.5
D1500	250	59.8
D2100	250	36.3
D2500	250	61.6
D2800	250	38.1

Table 12 Change of required minimum thickness of inner tubes with hollow ratio from modified equations for D1500

Hollow ratio	Thickness of inner tube (Han *et al*. 2010) (mm)	Thickness of inner tube (present) (mm)	Rate of reduction (%)
0.1	1.9	1.7	10.5
0.2	3.8	2.4	36.8
0.3	5.7	2.6	54.4
0.4	7.6	2.7	64.5
0.5	9.5	2.6	72.6
0.6	11.4	2.7	76.3
0.7	13.3	2.9	78.2
0.8	15.2	5.5	63.8
0.9	17.1	14.8	13.5

Additionally, the external confining stress was investigated via the application of the modified equations. As shown in Fig. 19, the external confining stress of each model is similar to the respective theoretical external confining stress. The differences between the stresses in the column models are less than 10%. Table 11 lists the von Mises stresses of the inner tubes in the models for which the hollow ratio is 0.8 when the outer tubes are in the yielding state. As shown in the table, the von Mises stresses of the inner tubes are significantly smaller than that of the outer tubes, indicating that the modified equation provides a high safety factor. The concrete sufficiently provided the triaxial confining effect by inserting the inner tube designed by the modified

equations.

Table 12 summarizes the required minimum thicknesses of the inner tubes as calculated by the modified equations and the equations from Han *et al*. (2010). The thickness of the inner tube calculated using the modified equations is 76% of the thickness calculated using the equation in Han *et al*. (2010). This proves that the modified equations can provide a more economical design of the inner tube as compared to the former equations under the same external confining stress in a DSCT column.

6. Summary and conclusions

In this paper, the internal confining stress in a DSCT column was investigated. Through this study, the difference between internal and external confining stresses was evaluated, and the relationship between the internal confining stresses was investigated using theoretical external confining stress and FEA. For presenting a rational design, modified equations for calculating the thickness of an inner tube in a DSCT column were proposed via numerical and mathematical solutions. The thickness of the inner tube was then calculated using the modified equations. The conclusions of this study are as follows:

(1) In the FEA models, both the damaged concrete plastic option and plastic option were applied to the concrete and steel in a DSCT column, respectively. Additionally, the frictionless option was used to consider the contact conditions between the concrete and the steel because the bonding stress between a steel tube and concrete is negligible. The obtained analysis results under these conditions were similar to the compared experimental test results. Therefore, the FEA method is useful for the inelastic analysis of composite structures without studs between the concrete and the steel tube.

(2) In an H-CFST column, the external confining stress rapidly decreases when the hollow ratio is greater than or equal to 0.7 as compared to the external confining stress of Han el al. (2010). This is due to a gradual reduction of the concrete area induced by the increase of the hollow portion. As the hollow ratio increases, the confining state of the concrete transforms from a triaxial confining state to a biaxial or uniaxial confining state.

(3) The evaluation of a DSCT column, which includes an inner tube in the core of an H-CFST column, resulted in an external confining stress that approached the value of the theoretical external confining stress. The internal confining stress was increased to increase the external confining stress. When the external confining stress is similar to the theoretical value, the concrete is under a triaxial confining state. Thus, an inner tube can be inserted in an H-CFST column for which the hollow ratio is greater than 0.6 in order to enhance the structural performance.

(4) In the results of the parametric study, the hollow ratio affects the internal confining stress of a DSCT column, while the other considered parameters rarely affect the stress. The relationship between the numerical internal confining stress and theoretical external confining stress was investigated via FEA. Using these results, regression analysis was used to determine the mathematical internal confining stress without the need for FEA. The relationship between the theoretical external confining stress and the mathematical confining stress was represented by the reduction coefficient, γ.

(5) The modified failure equations for the inner tube were based on the equations from Han *et al*. (2010). After the thickness of the inner tube was calculated by the modified equations, the failure modes of the inner tube were investigated using FEA models under various conditions. The

numerical internal confining stress values range from 70–90% of the mathematical internal confining stress values. The external confining stress values of each model are within 10% of their respective theoretical external confining stress values. Therefore, the mathematical internal confining stress values are slightly conservative as compared to the numerical internal confining stress values, ensuring a safe design.

(6) The thickness of the inner tube calculated using the modified equations is 76% of the thickness of the inner tube calculated using the equation in Han *et al*. (2010). This proves that the modified equations provide a more economical inner tube design as compared to the former equations under the same external confining stress in a DSCT column.

Acknowledgments

This research was supported by a grant (code 12 Technology Innovation E09) from the Construction Technology Innovation Program funded by the Ministry of Land, Transportation of the Korean government and a grant (PA110020) from the Patented Formula Commercialization Program, funded by the Seoul Business Agency.

References

ABAQUS Manual 6.9.1, SIMULIA, 2010

Andres, W.C., Oreta, Jason, M.C. and Ongpeng (2011), "Modeling the confined compressive strength of hybrid circular concrete columns using neural networks", *Comput. Concr.*, **8** (5), 597-616.

Bahrami, A., Hamidon, W. Badaruzzaman, W. and Osman, S.A. (2012), "Structural behaviour of tapered concrete-filled steel composite (TCFSC) columns subjected to eccentric loading", *Comput. Concr.*, **9**(6), 403-426.

Han, T.H, Stallings, J.M. and Kang, Y.J. (2010), Nonlinear Concrete Model for Double-Skinned Composite Tubular Columns", *Construct. Build. Mater.*, **24** (12), 2542-2553

Im, S.B., Han, T.H., Han, S.Y. and Kang, Y.J. (2006), Stress-strain relations of concrete according to the confining conditions, *J. Korean Soc.Civil Eng.*, **26**(4A), 743-52.

Kerr, A.D. and Soifer, M.T. (1996), The linearization of the prebuckling state and its effects on the determined instability load, *J. Appl. Mech.*, **36**(4), 775-85.

Rasheed, H.A., Abd El-Fattah, A.M., Esmaeily, A., Jones, J.P. and Hurst, K.F. (2012), "Software for adaptable eccentric analysis of confined concrete circular columns", *Comput. Concr.*, **10**(4),

Shakir-Khalil, H. and Illouli, S. (1987), Composite columns of concentric steel tubes. *In: Proceeding of Conference on the Design and Construction of Non Conventional Structures*, 73-82.

Shraideh, M.S. and Aboutaha, R.S. (2013), "Analysis of steel-GFRP reinforced concrete circular columns" *Comput. Concr.*, **11**(4),

Shrestha, R., Smith, S.T. and Samali, B. (2013), "Finite element modelling of FRP-strengthened RC beam-column connections with ANSYS" ,*Comput. Concr.*, **11**(1),

Tao, Z., Han, L.H. and Zhao, X.L. (2004), Behavior of concrete-filled double skin (CHS inner and CHS outer) steel tubular stub columns and beam columns, *J. Construct. Steel Re.*, **60**(8), 1129-58.

Tong, Z.S. and Lin, X.G. (2005), Basic Behavior of Centrifugal Hollow Concrete-filled Steel Tube (H-CFST) Stub Columns under Axial Compression. *Korea Society of Steel Construction*, **5**, 299-304.

Tsai, H.C. (2013), "Polynomial modeling of confined compressive strength and strain of circular concrete columns", *Comput. Concr.*, **11** (6),

Wei, S., Mau, S.T., Vipulanandan, C. and Mantrala, S.K. (1997), Performance of new sandwich tube under axial loading: Experiment, *J. Struct. Eng.*, **121**(12), 1806-1814.

Zhao, X.L. and Grzebieta, R. (2002), Strength and ductility of concrete filled double skin (SHS inner and SHS outer) tubes", *Thin-Walled Structures*, **40**(2), 199-213.
Zhu, W.C., Ling, L., Tang, C.A., Kang, Y.M. and Xie, L.M. (2012), "The 3D-numerical simulation on failure process of concrete-filled tubular (CFT) stub columns under uniaxial compression", *Comput.and Concr.*, **9**(4), 2012

CC